

Article

Interannual and Seasonal Variations in Ecosystem Transpiration and Water Use Efficiency in a Tropical Rainforest

Maricar Aguilos¹, Clément Stahl¹, Benoit Burban¹, Bruno Hérault^{2,3} , Elodie Courtois⁴, Sabrina Coste¹ , Fabien Wagner⁵, Camille Ziegler^{1,6}, Kentaro Takagi⁷ and Damien Bonal^{6,*}

¹ UMR EcoFoG, INRA, CNRS, Cirad, AgroParisTech, Université des Antilles, Université de Guyane, 97310 Kourou, French Guiana, France; maricar.aguilos@ecofog.gf (M.A.); clement.stahl@ecofog.gf (C.S.); benoit.burban@ecofog.gf (B.B.); sabrina.coste@ecofog.gf (S.C.); camille.ziegler@ecofog.gf (C.Z.)

² Cirad, UR Forests & Societies, Université de Montpellier, 34000 Montpellier, France; bruno.herault@cirad.fr

³ Institut National Polytechnique Félix Houphouët-Boigny (INP-HB), Yamoussoukro, Ivory Coast

⁴ Laboratoire Ecologie, évolution, interactions des systèmes amazoniens (LEEISA), CNRS, IFREMER, Université de Guyane, 97300 Cayenne, French Guiana, France; courtoiselodie@gmail.com

⁵ INPE, Av. dos Astronautas, SP 12227-010 São José dos Campos, Brazil; wagner.h.fabien@gmail.com

⁶ Université de Lorraine, AgroParisTech, INRA, UMR Silva, 54000 Nancy, France

⁷ Field Science Center for Northern Biosphere, Hokkaido University, Sapporo 060-0808, Japan; kentt@fsc.hokudai.ac.jp

* Correspondence: damien.bonal@inra.fr; Tel.: +33-3-83-39-73-43

Received: 10 November 2018; Accepted: 24 December 2018; Published: 26 December 2018



Abstract: Warmer and drier climates over Amazonia have been predicted for the next century with expected changes in regional water and carbon cycles. We examined the impact of interannual and seasonal variations in climate conditions on ecosystem-level evapotranspiration (ET) and water use efficiency (WUE) to determine key climatic drivers and anticipate the response of these ecosystems to climate change. We used daily climate and eddyflux data recorded at the Guyaflux site in French Guiana from 2004 to 2014. ET and WUE exhibited weak interannual variability. The main climatic driver of ET and WUE was global radiation (R_g), but relative extractable water (REW) and soil temperature (T_s) did also contribute. At the seasonal scale, ET and WUE showed a modal pattern driven by R_g , with maximum values for ET in July and August and for WUE at the beginning of the year. By removing radiation effects during water depleted periods, we showed that soil water stress strongly reduced ET. In contrast, drought conditions enhanced radiation-normalized WUE in almost all the years, suggesting that the lack of soil water had a more severe effect on ecosystem evapotranspiration than on photosynthesis. Our results are of major concern for tropical ecosystem modeling because they suggest that under future climate conditions, tropical forest ecosystems will be able to simultaneously adjust CO_2 and H_2O fluxes. Yet, for tropical forests under future conditions, the direction of change in WUE at the ecosystem scale is hard to predict, since the impact of radiation on WUE is counterbalanced by adjustments to soil water limitations. Developing mechanistic models that fully integrate the processes associated with CO_2 and H_2O flux control should help researchers understand and simulate future functional adjustments in these ecosystems.

Keywords: tropical rainforest; evapotranspiration; water use efficiency; drought; radiation

1. Introduction

The Amazon basin plays a crucial role in the regional and global climate system due to its large contribution to the global surface water and carbon cycle [1]. However, drier and warmer climates

over Amazonia have been predicted, due to climate change for the next 100 years [2], along with increasing drought frequency and severity. How tropical forests respond to these climate extremes is still an intense subject of debate [3–7].

Ecosystem evapotranspiration (ET) is an important component of the global water cycle and has a critical role in ecological and hydrological processes [8]. However, little is known about the mechanisms associated with the interannual variability of ET. While some ecosystem process models present ranges of interannual variability similar to those actually measured at flux towers (e.g., Soil-Plant-Atmosphere model [9]), others underestimate annual ET [9]. Deeper investigation into the factors determining the interannual variability of ET is therefore needed to address these discrepancies, particularly in tropical rainforests. Moreover, the seasonality of ET in the Amazon has been the subject of debate for over two decades. Field observations, flux measurements and modelling studies at multiple sites in Amazonian forests have generally shown higher ET rates during the dry season than during the wet season [10–15], thus indicating that the Amazon forest transpires more in the dry season.

In a changing environment, another major issue is how tropical rainforest ecosystems regulate and optimize the ratio between CO₂ assimilation (GPP, gross primary production) and evapotranspiration, as described by ecosystem water use efficiency (WUE). The equilibrium between assimilation and evapotranspiration reflects a set-point of foliar functioning and depends on how much the stomata of the tree open. Under limiting resource conditions (e.g., low radiation, lack of water), this equilibrium depends on the trade-off at the ecosystem level between limiting the rate of assimilation of CO₂ (benefit) and the transpiration speed (cost) [16]. Whether tropical rainforest ecosystems can adjust WUE over long time scales, particularly when soils are becoming drier, is a major question ecosystem models need to address.

Several factors have been found to control ecosystem ET and WUE. Many studies have reported that solar radiation enhances annual [17] or seasonal [10–12,18–20] ET rates. In contrast, hydraulic stress and/or stomatal control associated with depleted soil water restricts transpiration during drier conditions [21]. Yet, analyzing or simulating the drivers of WUE is more complex than meets the eye, since variations in WUE result from variations in ET and GPP, which can be decoupled. At the annual scale, ecosystem WUE was found to be positively correlated with radiation [22], precipitation [23] or temperature [24] in various tropical forest ecosystems. It should be noted that long-term trends for solar radiation and temperature do not vary much from year to year in the neo-tropical Amazon rainforest [25]. This means that fluctuations in soil water at the seasonal scale, brought about by changing rainfall patterns, may become predominant in determining the variations in the GPP/ET relationship. Studying the relations between climatic variables and water fluxes in the Amazon region may provide important new knowledge and reduce the uncertainty concerning the ecosystem's response to natural climate variations and possible extreme conditions in the future.

In this study, we used a single eddy flux dataset collected continuously over an 11-year period at the Guyaflux site in the tropical rainforest of French Guiana to determine the interannual and seasonal variations in ET and WUE and their climatic drivers. During the study period, from 2004 to 2014, the intensity and duration of seasonal droughts varied, thus allowing us to test the impact of various environmental factors (radiation, temperature, soil water stress) on ecosystem evapotranspiration and water use efficiency. Herein, we specifically discuss (1) the temporal variations in ET and WUE at the interannual and seasonal scales, including patterns during water depleted periods (WD), and (2) the environmental drivers of these variations. We expected strong interannual and seasonal variations in ET and WUE and hypothesized that radiation and soil water content would be the main drivers of these variations.

2. Materials and Methods

2.1. Study Site

The study was conducted at the Paracou research station in French Guiana, South America ($5^{\circ}16'54''$ N, $52^{\circ}54'44''$ W) in a tropical rainforest. Detailed information about the Guyaflux site where the flux tower is located is presented in [25] and [26]; here, we mention only the most important points. The climate shows large seasonal variations in rainfall [25]. Decadal (from 2004 to 2014) average annual rainfall at the study site was $3102 \text{ mm} \pm 70 \text{ mm}$ and the average annual air temperature was 25.7 ± 0.1 °C.

2.2. Climate and Flux Monitoring

Microclimate and eddy covariance data have been recorded continuously at the site since December 2003 ([25,26]) following the Euroflux methodology [27]. This study covers an 11-year period, from 2004 to 2014. Global and infrared incident and reflected radiation (CNR1, Kipp and Zonen, Bohemia, NY, USA) were measured above the canopy. Temperature sensors (CS107, Campbell Scientific Inc., Logan, UT, USA) were used to measure soil temperature (T_s , °C). A rain gauge (ARG100, EM Imt, Sunderland, UK) measured bulk rainfall above the canopy. Rainfall data were incorporated into a soil water balance model, developed and validated for the study site [28], to estimate relative extractable water (REW) for trees from the soil surface down to 3-m in depth. REW is a dimensionless variable that characterizes the water status of the soil at a given date relative to its maximum potential soil water content.

Dataloggers (CR23X, CR1000 or CR3000, Campbell Scientific Inc., Logan, UT, USA) were used to collect meteorological data at 1 min intervals and to compile them as 30 min averages or sums. The 30-minute data were summed for rainfall and averaged for the other parameters to obtain daily values. Our objective was to focus on the impact of these meteorological data on evapotranspiration and water use efficiency while the canopy was fully active and under rather stable climate conditions. We thus eliminated nighttime, early morning or early evening periods. We thus only considered meteorological data taken during the period from 10:00 am to 16:00 pm, except for daily rainfall and REW, which were summed or averaged for 24 h a day.

We used a 3-D sonic anemometer (R3-50; Gill Instruments, Lymington, UK) to measure wind velocities and sonic temperature at 20 Hz. We used to an open-path infrared gas analyzer (Li7500, LI-COR Inc., Lincoln, NE, USA) to monitor CO_2 and H_2O concentrations at 20 Hz. As the open-path gas analyzer proved to be very sensitive to rain, a closed-path infra-red gas analyzer (Li7000, LI-COR Inc., Lincoln, NE, USA) was added to the system in June 2005 to gap-fill the missing data from the Li7500 analyzer. Eddy covariance data were saved with the EDDYLOGP software (Alterra, Wageningen, The Netherlands) on 256 MB memory cards inserted into an HP200LX laptop (Hewlett Packard, Palo Alto, CA, USA) and downloaded weekly to another computer.

2.3. Daytime Evapotranspiration (ET)

Water loss by evaporation at the ecosystem level during the daytime was determined from 30-min values of the flow of latent heat (LE , W m^{-2}) obtained with the eddy flux system. Based on these data, we calculated daily daytime ET ($\text{kg H}_2\text{O m}^{-2} \text{ d}^{-1}$) as the average of the LE data during the daytime (10:00–16:00). We filtered 393 (9%) daytime outliers out of the total 4018 ET data points available when daytime R_g was lower than 150 W m^{-2} following [29], or when daytime LE was lower than 50 W m^{-2} . We did not gap-fill any missing data after filtering.

2.4. Water Use Efficiency (WUE)

Ecosystem WUE was defined as the ratio of GPP to ET according to [30,31]. To estimate daytime WUE ($\text{g C kg H}_2\text{O}^{-1}$), we used daily daytime averages for GPP ($\text{g C m}^{-2} \text{ d}^{-1}$) and ET ($\text{kg H}_2\text{O m}^{-2} \text{ d}^{-1}$)

calculated from half-hourly measurements. Daily GPP raw data were extracted from a previous study [28]. No further filtering on WUE was done.

2.5. Soil Water Stress Index (SWSI) and the Water Depletion Period

In order to determine the impact of water depletion on ET and WUE, an eco-hydrological drought indicator called the soil water stress index (SWSI) was calculated [32]. SWSI is a dimensionless number that is calculated as the difference between the daily REW value and 0.4 (a threshold value for REW that induces stomatal closure in most trees), divided by 0.4. Therefore, at field capacity (REW = 1), SWSI equals 1.5; at wilting point (REW = 0), SWSI equals -1 ; SWSI equals 0 when REW = 0.4.

To test the effect of soil water limitation on ET and WUE, we selected the period when REW drops from 1 down to its minimum value within the July–December window (Figure 1). This period is hereafter referred to as the water depleted (WD) period. SWSI of each year (SWSI_a) was calculated as the algebraic sum of daily SWSI values during the WD period.

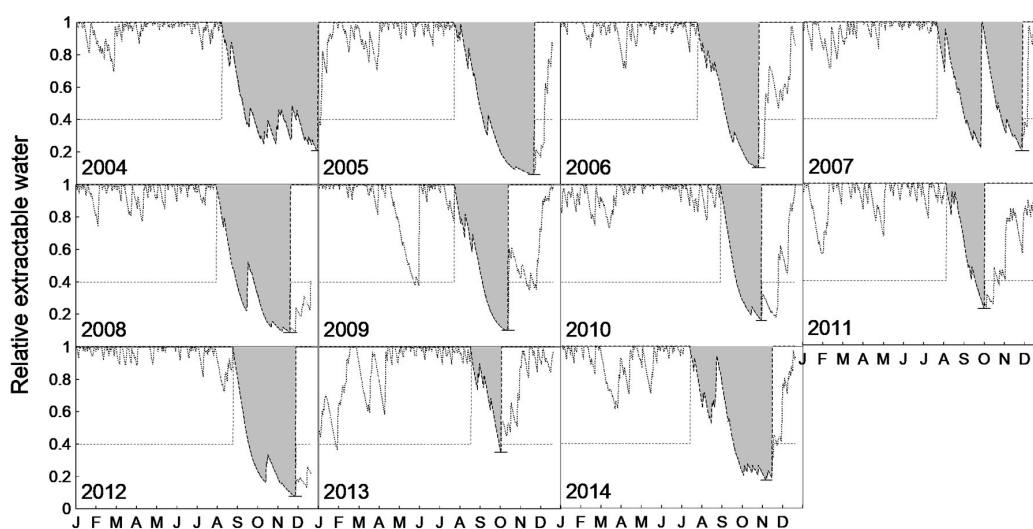


Figure 1. Seasonal variations in relative extractable water (REW) for each year (2004–2014). The water depletion period (WD, gray shaded area) is characterized by REW dropping from its field saturation point (REW < 1~0.4, dotted line), passing through its threshold level (REW = 0.4, short thin straight dashed line), down to its lowest point (solid line at the bottom of the lowest REW level).

2.6. Data Analyses

2.6.1. Normalizing ET and WUE

To analyze soil drought effect alone, we normalized ET and WUE with global radiation (R_g). Indeed, from September to December, R_g decreases because of the Earth's axial tilt and the presence of clouds. To eliminate this potential effect on ET and WUE and test the direct effect of soil water limitation, linear models were created to determine residuals from the relationships between ET or WUE and R_g. These residuals were used to analyze the relationship between R_g-normalized ET or WUE and SWSI during the WD period.

2.6.2. Isolating the Most Important Climate Variables

We used the Principal Component Analysis (PCA) procedure described in [25] to reveal the main climate gradients of the dataset while reducing multicollinearity problems among the tested climatic variables (global radiation (R_g), relative extractable water (REW), vapor pressure deficit, rainfall, soil temperature (T_s), air temperature, evapotranspiration, relative humidity and water balance index).

2.6.3. Ecosystem Response to Climatic Drivers

As described in [25], we built generalized additive models with spline smoothers to predict ET and WUE as a function of the PCA-selected climate variables. We used the gam function from the mgcv package to build the models and the MuMin package to obtain the best smoothing dimension. Spline term effects were ranked according to their F-values (Wald tests). Standardized major axis (SMA) regressions performed with the smatr package in R were used to test the relationship between soil water stress index and Rg-normalized ET or WUE. Smooth curve fitting was carried out with a locally weighted polynomial regression in the ggplot2 package. We analyzed the contribution of ET and GPP to WUE (variance partitioning) with a general function and used the propagate package to calculate uncertainty propagation by Taylor expansion and Monte Carlo simulation. All analyses were processed in R version 3.4.2 (Vienna, Austria).

3. Results

3.1. Interannual Variations in ET, WUE and Climate

Over the 11-year period, ET and WUE exhibited significant interannual variability ($p < 0.001$) (Figure 2). The amplitude of the interannual rate of change was 10.4% and 15.8% for ET and WUE, respectively. There was a significant coupling of ET and GPP (data from [25]) ($R^2 = 0.35$; $p < 0.001$). Propagating GPP and ET variability into WUE, we found that 39.6% of the variance for WUE came from GPP and 60.4% from ET.

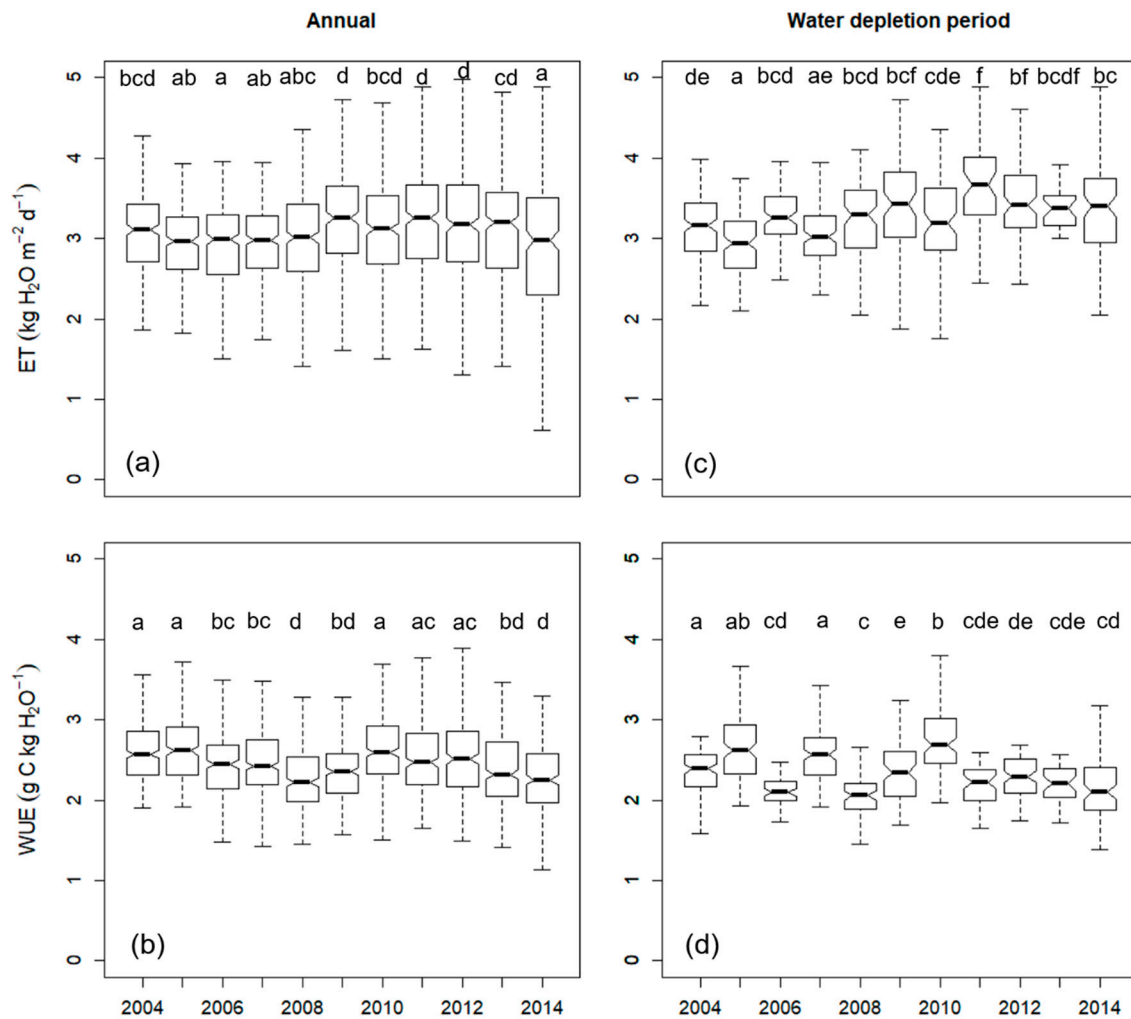


Figure 2. Interannual variations in ecosystem evapotranspiration (ET) (a) and (c) and water use efficiency (WUE) (b) and (d) at the whole year scale (left) and during water depletion (WD) periods (right). Daily data from 2004 to 2014 were used. In the boxplots, the thick line shows the median; the box extends to the upper and lower quartiles; and dashed lines indicate the nominal range. For a given graph, different letters denote significant differences among years ($p < 0.05$).

Inter-annually, radiation, temperature, wind speed and air humidity varied little at the study site (2 to 12% variations between the minimum and maximum values) (Figure 3). Interannual variations in REW and rainfall were stronger (19% and 16%, respectively). Years with highly negative total water stress indicator values (ie. severe water stress and long droughts) include 2005 (SWSIa = -5.06), 2008 (SWSIa = -2.11), 2010 (SWSIa = -5.64) and 2012 (SWSIa = -17.37) (Table 1 and Figure A1).

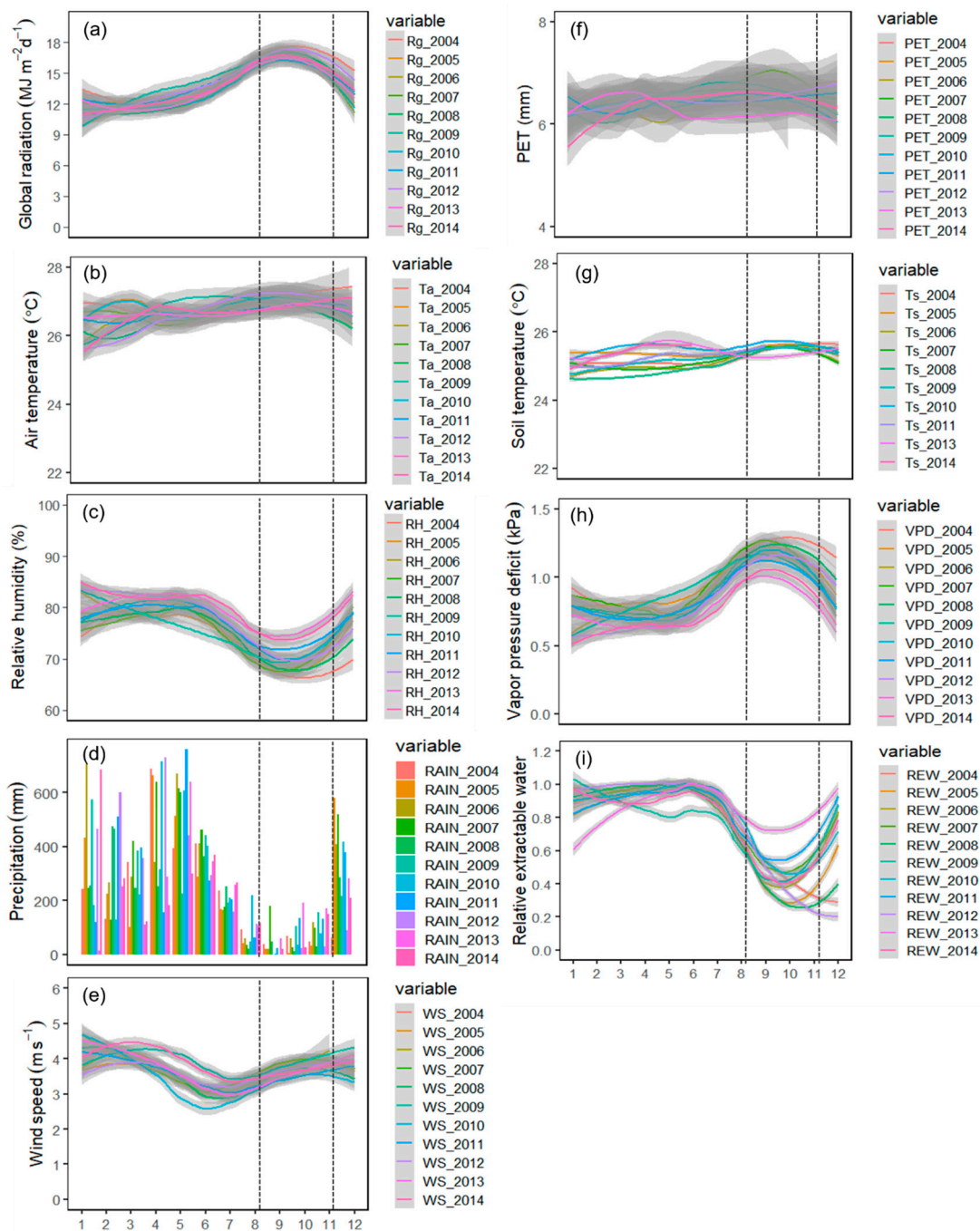


Figure 3. Interannual and seasonal variations for climate variables. (a) Global radiation (R_g , $\text{MJ m}^{-2} \text{d}^{-1}$), (b) Air temperature (T_a , $^{\circ}\text{C}$), (c) Air relative humidity (RH, %), (d) Precipitation (Rain, mm), (e) Wind speed (WS, m s^{-1}), (f) Potential Evapotranspiration (PET, mm), (g) Soil temperature (T_s , $^{\circ}\text{C}$), (h) Vapor pressure deficit (VPD, kPa), (i) Relative extractable water (REW, unitless). Different colors were assigned for each year. Gray-shaded regions are the confidence intervals and the colored line in the grayscale line is the smooth curve. The two vertical broken lines in each panel represent the average day of the year for the beginning and end of the WD period. Monthly sums for precipitation in (d) are presented in a bar plot.

Table 1. Annual soil water depletion duration, annual sum of soil water stress index (SWSIa) during the water depleted period, and annual minimum REW from 2004–2014.

Year	Soil Water Depletion Duration (no. of days)	SWSIa	Minimum REW
2004	143	13.2	0.21
2005	119	−5.60	0.06
2006	91	11.29	0.10
2007	127	40.04	0.20
2008	110	−12.11	0.09
2009	80	11.13	0.10
2010	83	−5.94	0.16
2011	57	29.97	0.23
2012	93	−17.37	0.08
2013	45	32.89	0.35
2014	122	26.65	0.17

Years with the most severe drought conditions during the water depleted period are indicated in bold.

Global radiation (Rg), relative extractable water (REW) and soil temperature (Ts) were the three meteorological parameters that best represented the main climate gradients in our dataset. On an annual basis, Rg appeared to be the best climate predictor for ET ($R^2 = 0.70$; $p < 0.001$) and WUE ($R^2 = 0.40$; $p < 0.001$) (Table 2). REW and Ts were the second- and third-best predictors for both ET and WUE.

Table 2. Results of the generalized additive model (GAM) analysis done to detect the best models and rank predictor variables (Rg, REW, Ts) according to their ability to explain variations in ET and WUE, annually and during the soil W) period, from 2004–2014. Daily data was used in the analysis. *F*-values and *p*-values are statistics given by the GAM analyses.

Period/ Dependent Variable	Best Model Predictors	Multiple R^2	Intercept	Coefficients		<i>F</i> value	<i>p</i> Value
				1	2		
Annual ET	Rg	0.70	2.92	0.46	0.71	1112.9	<0.001
	REW			0.20	0.22	102.7	<0.001
	Ts			0.06	0.04	6.8	<0.001
WUE	Rg	0.40	2.68	−0.57	−0.54	164.0	<0.001
	REW			0.09	−0.08	6.9	<0.001
	Ts			−0.17	−0.02	2.5	<0.050
Water depletion (WD) period ET	Rg	0.48	3.19	9.51	3.39	180.6	<0.001
	REW			1.01	2.20	105.3	<0.001
	Ts			−0.16	−0.29	86.9	<0.001
WUE	Rg	0.34	2.48	−0.12	0.08	21.9	<0.001
	Ts			−0.12	0.08	21.9	<0.001

3.2. Seasonal Variations in ET, WUE and climate

A gradual increase in Rg was observed from January to September/October, followed by a rapid slowdown towards the end of the year (Figure 3). In contrast, REW coincided with precipitation patterns: REW remained rather constant from January to July and slowed down as the dry season (water depleted period) began, with its lowest levels occurring in October/November (except for 2004). REW picked up again as the rainy season started towards the end of November. Like REW, air humidity and vapor pressure deficit (VPD) remained constant from January to June. Air humidity then decreased and reached a minimum in September. In contrast, the VPD increased from June to

October. Wind speed was usually lower during the wet season, i.e., around May and June. Air or soil temperature remained relatively constant all year round.

Each year, we observed opposing seasonal patterns between ET and WUE (Figure 4). ET increased at the beginning of the year, peaked in August, and gradually declined towards November. In contrast, the lowest WUE values were observed around mid-August and picked up slightly around the end of the year, after major rain events returned (Figure 4).

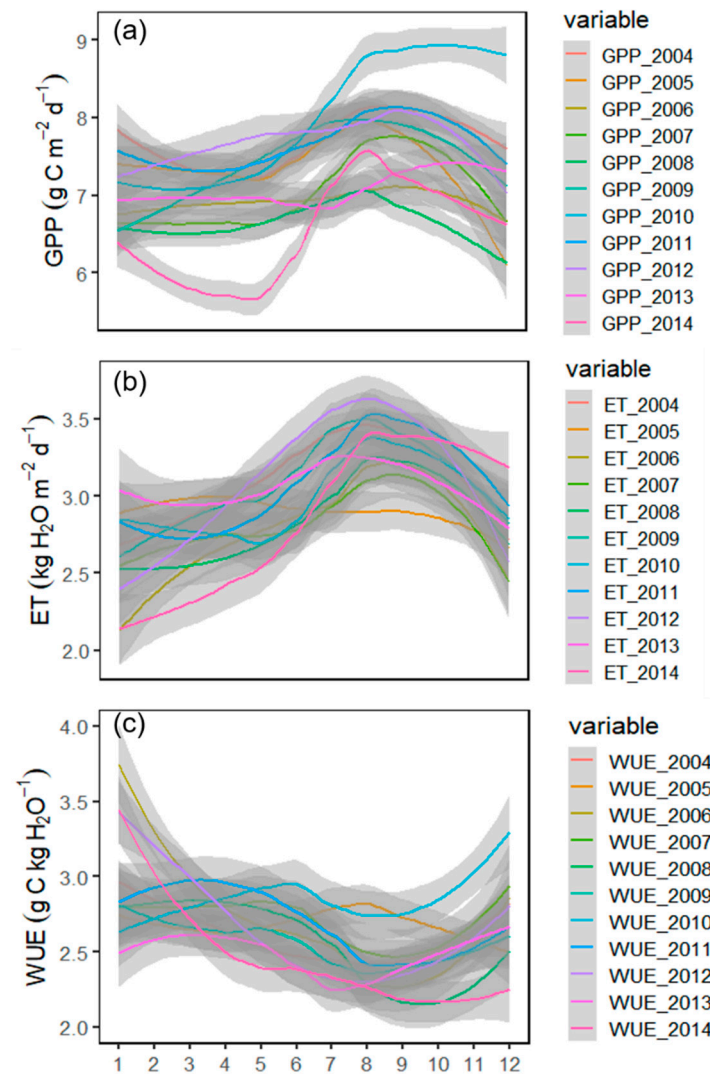


Figure 4. Seasonal variations (monthly means) in (a) ecosystem gross primary production (GPP), (b) ecosystem evapotranspiration (ET), and (c) ecosystem water use efficiency (WUE) based on daily smoothed values for each year from 2004–2014. Different colors were assigned for each year. Gray-shaded regions are the confidence intervals and the colored line in the grayscale line is the smooth curve. The two vertical broken lines in each panel represent the average day of the year for the beginning and end of the water depletion (WD) period. GPP data are from [25].

3.3. Variations in ET and WUE during the Water Depletion (WD) Periods

There was an overall 9.3% increase in ET during the WD period (August–November) as compared to the whole year (Figures 2 and 4). In contrast, WUE was 8.2% lower during the WD period as compared to annual values (Figures 2 and 4). Within the WD period, we found a 4%–18% rate of decrease in ET, except in 2005 when a negligible decline was observed (Figure 4). In contrast, WUE

increased by 1%–17%, except in 2005 and 2014, when a slight decrease was observed during the WD period (Figure 4).

During WD periods, the combined effect of R_g and REW drove 48% of the variability in ET (Table 2); yet, R_g was the primary controlling factor. There was no effect of T_s on ET during the WD periods (Table 2). There was a positive relationship between R_g -normalized ET and SWSI for each year (Figure 5). These linear relationships differed among years; the slopes were much higher in the years 2004, 2008 and 2012–2014, and these slopes were all statistically different from those for 2005 and 2006 (Tables A1 and A2).

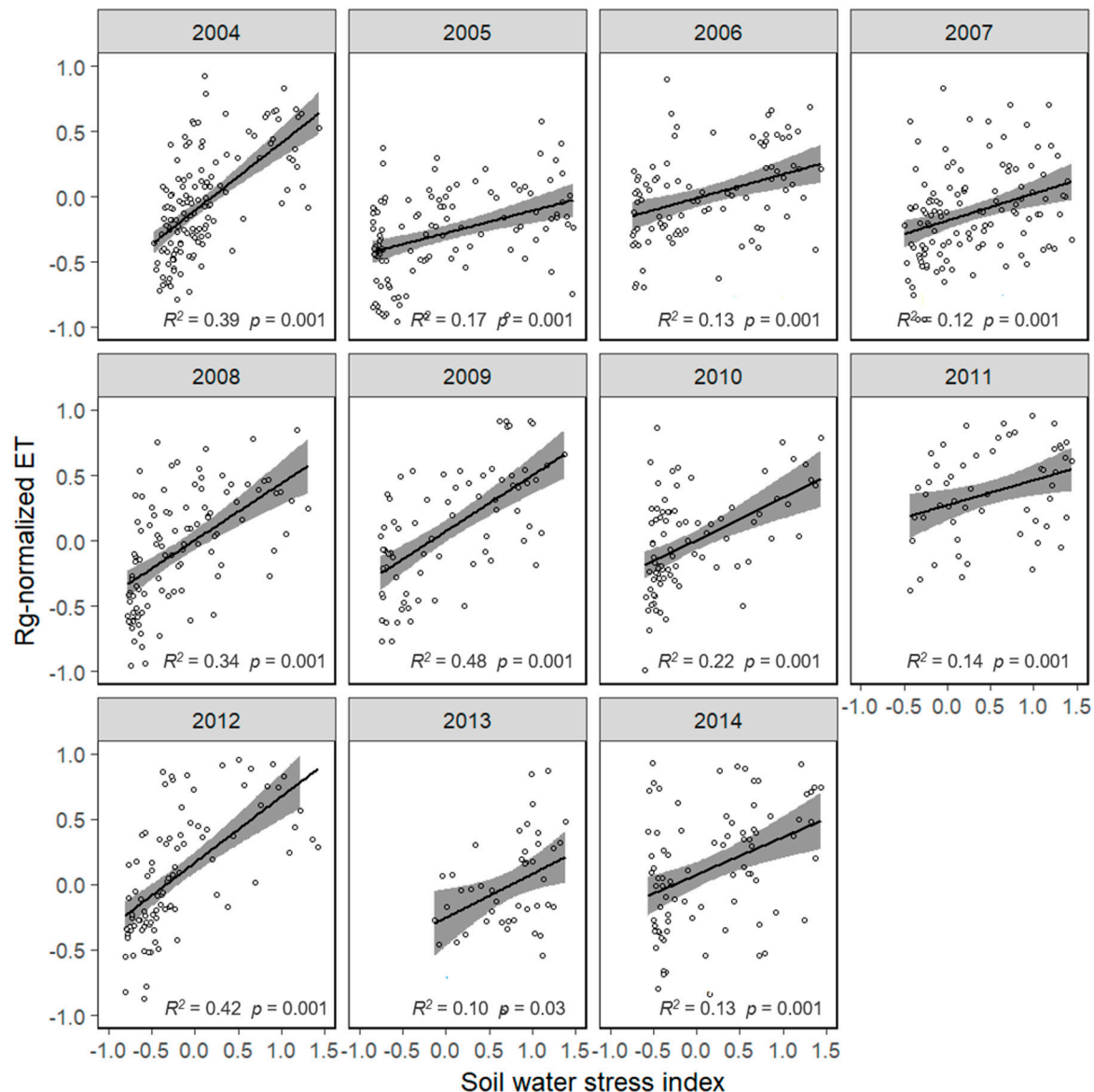


Figure 5. Linear relationship between radiation-normalized evapotranspiration (ET) and soil water stress index (SWSI) during the water depletion period (WD). Gray-shaded regions are the confidence intervals and the black line in between is the linear trend. Each dot corresponds to one day. The greater the SWSI, the lower the soil water stress.

Variations in WUE during WD periods were also driven by R_g , with a slight influence of T_s (Table 2). REW had no control over WUE. The relationship between R_g -normalized WUE and SWSI differed among years (Figure 6). We observed no relationships between the two variables in 2008, 2011,

and 2014, whereas the relationships were negative in 2004, 2006, 2007, 2009, 2010, 2012 and 2013, and positive in 2005.

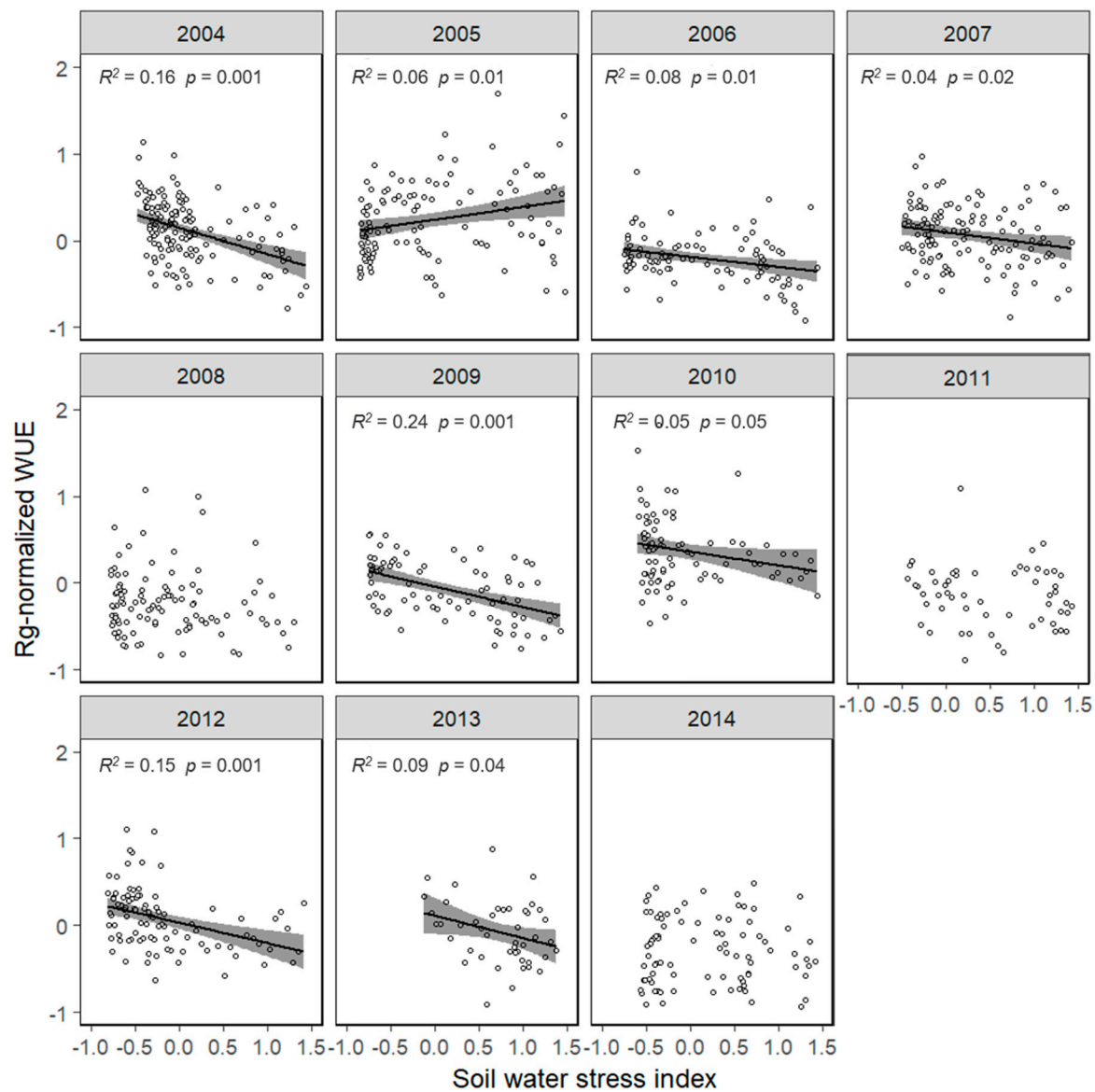


Figure 6. Linear relationship between radiation-normalized water use efficiency (WUE) and the soil water stress index (SWSI) during the water depletion period (WD). Gray-shaded regions are the confidence intervals and the black line in between is the linear trend. Each dot corresponds to one day. The greater the SWSI, the lower the soil water stress.

4. Discussion

4.1. Interannual Variations in ET and WUE

Many studies in the Amazon have addressed aspects of seasonal variations in ET; yet little information is available on ET interannual variability, especially over long time scales. In this study, annual mean ET was $2.95 \text{ kg H}_2\text{O m}^{-2} \text{ d}^{-1}$ (95% CI (2.93, 2.98)), which is within the range of values found in other studies conducted in Amazonia (Table 3). We found a 10.4% year-to-year variation in ET within the 11-year period. This variation is low and consistent with the 5%–10% variations previously observed in an Amazonian forest [18], but is lower than in tropical forests outside the

Amazon. For example, subtropical forests in Malaysia and China showed between 10% and 25% variability [1,17,33,34].

Annual mean WUE was $2.65 \text{ g C kg H}_2\text{O}^{-1}$ (95% CI (2.62, 2.67)) and interannual variations in WUE were low (15.8%). WUE-related literature on tropical forests is scarce (unlike for ET) [35] and this makes a comprehensive comparison of WUE values difficult. Yet, our year-to-year variations in WUE were much lower compared to the 35% variability found in a subtropical forest in China [34]. A decline in leaf WUE has been observed since the 1950s in many studies, associated with the functional response of foliage to increasing atmospheric CO_2 concentrations and ^{13}C enrichment of atmospheric CO_2 (e.g., [36]). We did not observe any such decreasing trend at the ecosystem level for our study period. As ecosystem-level WUE results from the integrative mean of leaf-level tree WUE, interspecific variability in the response of trees to these CO_2 changes could also be an explanation. In any case, the interannual variability in WUE we observed suggests that, although annual ET and GPP respond to the same primary climate drivers (Table 2 and [25]), the extent of their responses varies among years. Furthermore, the combined effect of radiation, soil water and temperature only explained 40% of the between-year variance in WUE; biological control mechanisms may also be playing a major role at this time-scale. Inherent rhythms of leaf phenology [37], structural changes in vegetation [38], major mortality events [39], changes in surface conductance mediated by stomata [10] or the consequences of forest disturbance [1], both individually or in combinations do affect WUE and could very well be involved in these year-to-year variations. Long-term monitoring of these biological mechanisms is needed at eddy flux tower sites to assess their potential contribution to WUE.

Table 3. Comparison of evapotranspiration (ET) in various studies from the Amazon and other tropical forests.

Location/Ecosystem	Study Period	Interannual Variations in ET (%)	Daily Average ET ($\text{kg H}_2\text{O m}^{-2} \text{d}^{-1}$)		References
			Annual Period	Water Depletion Period	
Southern Brazil, Amazon	2000–2002	5–10		2.7	[18]
Tropical forests mostly Amazon (modelling study)			3.75		[19]
Amazon forests	1996–2006				[13]
-Manaus				3.3–3.9	
-Santarem				3.3–3.9	
-Jaru				1.3–3.3	
-Javaes				1.3–3.3	
-Sinop				1.3–3.3	
-Pe de Gigante				1.3	
Eastern Amazon	2000–2001		3.51	3.96	[40]
Amazon					[10]
-Manaus	1999–2000		3.58	3.70	
-Santarem	2000–2003		3.49	3.59	
-Jaru	2000–2003		3.57	3.27	
-Sinop	2004–2005		3.11	3.18	
Amazon forest, Brazil	2002–2006	18	2.4–3.76	3.41	[17]
Sub-tropical forest in China	2003–2005	15.5	2.62		[34]
Tropical forest in Malaysia	2000–2009	12	3.62		[33]
Tropical forest in French Guiana	2004–2014	10.4	2.95	3.23	This study

4.2. Seasonal Variations in ET and WUE

There was a strong seasonal pattern for both ET and WUE (Figure 4). ET showed a minimum value at the beginning of the year and reached a maximum around August (Figures 2 and 4); these seasonal variations could be driven by climatic conditions either directly or indirectly, through their effect on biotic mechanisms, such as leaf phenology. What precise functional mechanisms explain why ET is elevated during seasonal dry periods? First, several studies conducted in the Amazon region have reported that ET is mainly driven by global radiation, both annually [1,10,19] and during

seasonal dry periods [10–12] and R_g was indeed the main driver of seasonal variations in ET at our site (Table 2). High monthly radiation can be reached either when cloud cover is low during the dry season or when the Earth's axial tilt maximizes incident solar radiation at this latitude (i.e., at the end of March and the beginning of September). During these periods of high R_g , the large amount of solar energy induces strong evaporative demand resulting in high ecosystem evapotranspiration rates [10–13,18–20]. Second, at the ecosystem level, the potential reduction in leaf transpiration by stomatal closure is compensated for in part by dry air entrainment from above the boundary layer and by changes in leaf temperature [41], meaning that canopy evaporation may not be reduced despite stomatal closure. Third, tropical rainforests can continue transpiring during periods of limited precipitation, because canopy trees are able to use available water from deep soil layers, thanks to a deep rooting system [42,43]. Hydraulic redistribution and upward soil capillary water flux may also help sustain ET during the dry season [39,44], though such mechanisms have not been documented at our study site [42]. Fourth, the seasonal dynamics of leaf emergence and leaf fall (i.e., leaf phenology) has also been suggested as a possible explanatory mechanism for the dry-season maxima of carbon and water fluxes in tropical forests [17,45], with leaf fall together with new leaf emergence peaking at the onset of the dry season. All of these patterns may, in one way or another, have contributed to the increase in ET during the WD period at our site.

The seasonal pattern for WUE was different from that of ET. We expected a lesser decrease in ET than in GPP during water deficit conditions (WD period), which would lead to higher WUE. Actually, the opposite pattern clearly occurred. Within any given year, the WD period had the lowest WUE values (on average, 7.6% lower than during the rest of the year; 1%–17%) (Figure 4). Subtropical forest ecosystems in China suffering from frequent drought also showed lower WUE during dry periods [24]. A decline in WUE with drought in semi-arid/sub-humid ecosystems was also reported in an overview [31], where a decrease in ET that was smaller than the GPP response during the dry period led to lower WUE in drier years. Seasonal variations in WUE are complex and difficult to analyze, since WUE results from a trade-off at the ecosystem level between water loss and carbon gain, and numerous factors affect these fluxes, and to different extents. Divergent patterns in WUE have indeed been revealed under contrasted soil water conditions. In a study of a long-term, extreme, experimental drought [9], the increase in WUE was indeed caused by a stronger decline in ET than in GPP; yet, the observed pattern was different in the control treatment (no rain exclusion) where the moderate decline in soil water availability did not actually affect ET. We show that the decrease in WUE during WD periods was the result of both an increase in ET (this study) and GPP ([25]), but to different degrees (rates of 4%–18% for ET and 2%–10% for GPP, [25]). The observed reduction in WUE during the WD period as compared to the rest of the year cannot be solely explained by expected patterns of change in ET and GPP when environmental conditions become extremely dry. Indeed, the decrease we found was driven mainly by light availability (Table 2) and by a greater positive effect of increased radiation during the WD period on GPP than on ET. This result is consistent with previous modeling approaches pointing out that tropical rainforests are mainly light-limited rather than water-limited [46] and that radiation is a major driver of both ET and WUE [35]. The asynchronous response of GPP and ET illustrates the decoupling that can occur between carbon and water cycles in this ecosystem. Simulations of tropical rainforest ecosystem responses to climate change should include this decoupling to better predict carbon and water cycling at the planetary scale.

4.3. Variations in ET and WUE within the WD Period

The impact of seasonal drought on ET in tropical forest ecosystems was found to be inconsistent among studies (Table 3). During water depleted periods, evapotranspiration of tropical rainforests was found to be reduced due to stomatal closure resulting from limited soil water content [10,24]. However, other studies claim that ET is greater during seasonal water depleted periods [13–15,19], pointing out that the positive effect on ET of increased solar radiation during seasonal dry periods was greater than the possible negative effect of soil water limitation. At our site, strong variations in ET (25%) occurred

during the WD period (Figure 4). In general, ET was highest at the beginning of the WD period, then linearly decreased during the period, clearly indicating that the changing environmental conditions during the seasonal dry period had a negative effect on ecosystem transpiration.

A combination of different abiotic drivers may explain this pattern. During the WD period, R_g decreased over time, mainly because of the rotation of the earth, while relative water content strongly decreased because of reduced rainfall (Figure 3). This combined decrease in R_g and REW may have induced a decrease in ET during the WD periods. Yet, R_g was found to be the strongest predictor of ET during the WD periods over the 11 years (Table 2). Air humidity also varied during the dry season (Figure 3) and the decrease in vapor pressure deficit could also have contributed to the decrease in ET. Stronger stomatal control during the day when air humidity is low and vapor pressure deficit is high can indeed result in lower ET. However, this potential impact was impossible to disentangle from the impacts of R_g and REW (see PCA on climatic factors in [28]). When the effect of reducing solar radiation from September to November was removed to analyze soil water effect alone (Figure 5), R_g -normalized ET exhibited a strong sensitivity to water stress, which was proportional to WD intensity, with lower evapotranspiration occurring when soil water content worsened. This occurred because low REW, likely linked to water demand approaching or exceeding supply, induced stomatal regulation to restrict transpiration [21]. As drought conditions became harsher, the sensitivity of transpiration to water deficit was stronger, suggesting a predominant down-regulation of stomatal conductance, which lowered tree transpiration under extreme droughts.

It is noteworthy that interannual variations in the intensity and the duration of the WD period at our site (Figure 1) caused in-between-year R_g -normalized ET slopes to differ significantly (Table A1), except in 2007, 2010 and 2011 (Table 1). This indicates that soil water stress levels induce different levels of evapotranspiration change when radiation is not limiting. This year-to-year variation in the slopes between R_g -normalized ET and SWSI may have occurred because, at the tree level, while some species may have suffered from the drought conditions, others some may not have, depending on drought intensity levels [47,48].

Within the WD period, variations in WUE were low (Figure 4) and the variations observed were not consistent among years (Figure 4). We did not expect this pattern, owing to the large variations in ET (Figure 4) and GPP [25] observed during the WD period at this site. Yet, as WUE represents a trade-off between these two fluxes at the ecosystem level, the absence of major variations in WUE during the WD period confirms that, even though all the processes involved in the carbon and water fluxes may vary individually, all together they converge towards rather stable water use efficiency. This is a very important result for ecosystem modeling as it suggests that, despite strong variations in environmental factors and carbon and water fluxes during water depleted periods, ecosystem WUE can be parameterized with a constant value during water depleted periods in these models.

A wealth of literature is available on the climatic drivers of ET and GPP, but to date, information about drivers of WUE during drought periods in tropical forests have been wanting. In our long-term study, we found that the weak variations in WUE observed during the WD periods were mainly controlled by global radiation and soil temperature, not by soil water (Table 2). In contrast to the effects of R_g on ET and GPP, R_g explained little of the variability of WUE during the WD period (Table 2). However, the R_g /WUE relationship was negative. This suggests that under future climate conditions with longer WD periods, less cloudy conditions, higher CO_2 concentration, and greater solar radiation [2], tropical forest ecosystems may adjust their CO_2 and H_2O flux control and become less efficient, transpiring a greater amount of water as compared to the CO_2 absorbed for growth. Such a scenario must be considered with great care, however, as, again, the observed variations in WUE during WD periods were very low.

When the influence of R_g on WUE during the WD periods was removed (R_g -normalized WUE), the decrease in REW induced a slight increase in normalized WUE for most WD periods (Figure 6). Such a pattern of normalized WUE increasing with soil water deficit is consistent with the general literature on WUE/soil water content effects [23,44]. The observed diverging effects of R_g and soil

water content on WUE during drought periods once again illustrates the complexity of the drivers of seasonal variations in WUE and the challenges that must be overcome before ecosystem process models will be able to precisely simulate these variations. The origin of the patterns we found can be discussed based on our knowledge of leaf-level responses of CO₂ and H₂O exchanges to drought. At leaf level, stomatal closure during drought usually induces a stronger down-regulation of transpiration than of photosynthesis [47]. Photosynthesis is usually reduced less than transpiration during severe dry conditions, since transpiration is linearly related to stomatal conductance, whereas photosynthesis may be limited by a variety of other factors and does not respond linearly to instantaneous changes in stomatal conductance [49]. The decline in Rg-normalized WUE during water depleted periods suggests that these mechanisms might indeed drive the observed ecosystem-level patterns observed at our site.

5. Conclusions

This study enriches the scarce literature on what drives short- and long-term variations in ecosystem evapotranspiration and WUE in tropical rainforests and contributes to improving the structure and calibration of ecosystem models and to a better understanding of vegetation-climate feedback loops in the tropics [35]. We present current trends on how well tropical rainforest ecosystems effectively utilize available solar radiation and respond to limited soil water during water depleted periods. Interannual variations in ET and WUE remained low whereas seasonal variations were strong. As for carbon fluxes, solar radiation was the major driver of variations in water consumption and water use efficiency at the different time-scales we considered. Yet, removing the solar radiation influence and directly investigating the influence of soil water availability during water depleted periods revealed differing response patterns of normalized ET and WUE to water deficit. Our results suggest that the lack of soil water has a more severe effect on ecosystem evapotranspiration than on ecosystem productivity, and that the ecosystem must have adjusted its fluxes to reduce water use when soil water is limiting. We also found that the response of ET to drought is dependent on the severity and duration of the water depletion period, as part of the tree community in this ecosystem may or may not be affected by drought. On the other hand, the greater the solar radiation, the lower ecosystem WUE became, suggesting that enhanced radiation during the dry season induced a greater increase in ET than in GPP.

These results are of major concern for tropical ecosystem modeling, because they imply that under future climate conditions in this region, tropical forest ecosystems may adjust their CO₂ and H₂O flux control. Yet, the direction of the future change in WUE at the ecosystem scale for tropical rainforests is hard to predict since the impact of increased radiation and soil water limitations on WUE can be divergent. Furthermore, the impact of long-term changes in temperature and atmospheric CO₂ concentrations, which are both expected to rise beyond the interannual variations explored here, will also interact with these effects. Developing mechanistic models that fully integrate the processes associated with CO₂ and H₂O flux control from tropical rainforest sites should help us understand and simulate future functional adjustments in these ecosystems. Our results reveal that changes in H₂O fluxes at this tropical forest site during seasonal dry periods directly reflected the down-regulation of these fluxes at leaf-level, as if ecosystem functioning was simply the additive functioning of single-tree or single-species in this ecosystem. A potential change in species composition of these ecosystems in the future, due to climate change will then surely impact CO₂ and H₂O flux control of these ecosystems. Confirmation of similar patterns from other tropical sites would be helpful before simplifying any up-scaling and modeling efforts.

Author Contributions: Conceived and designed the experiments: M.A., B.B., and D.B.; Data acquisition: B.B., and D.B.; Analyzed the data: M.A., C.S., B.H., E.C., K.T., C.Z., and D.B.; Contributed materials/analysis tools: F.W.; Wrote the paper: M.A., C.S., S.C., B.H., E.C., C.Z., and D.B.; All authors read and approved the final manuscript.

Funding: This study was carried out as a part of the Guyaflux program funded by the French Ministry of Research, INRA, CNES and co-funded by the European Regional Development Fund (FEDER, 2007–2013). The Guyaflux

program is a member of the SOERE F-ORE-T, which is supported annually by Ecofor, Allenvi and the French national research infrastructure, ANAEE-F (ANAEE-France: ANR-11-INBS-0001). This study also received support from the “Observatoire du Carbone en Guyane” and two “investissement d’avenir” grants from the Agence Nationale de la Recherche (CEBA, ref ANR-10-LABX-25-01; ARBRE, ref. ANR-11-LABX-0002-01).

Acknowledgments: We are grateful for the assistance of Jean-Yves Goret and Jocelyn Cazal in gathering the data. We thank J. Elbers (Wageningen University, The Netherlands) for the ALTEDDY software.

Conflicts of Interest: The authors declare no conflict of interest.

Appendix A

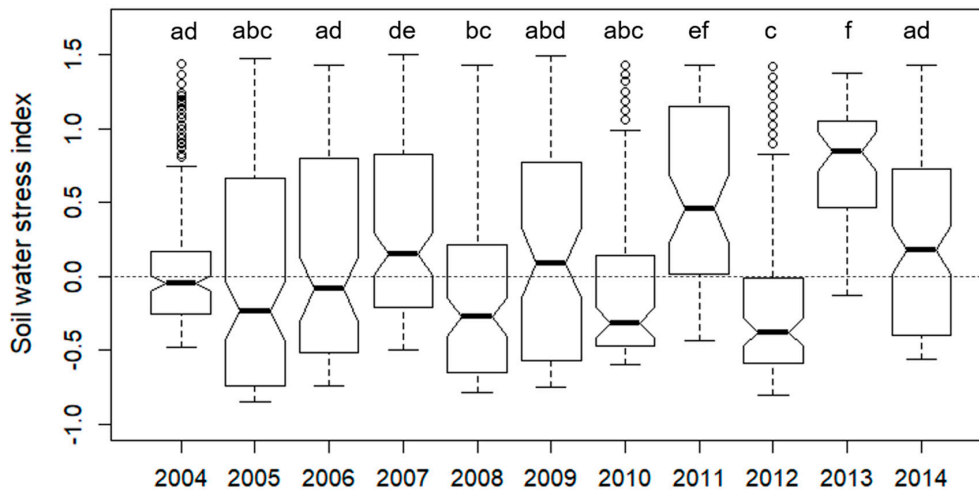


Figure A1. Interannual variations in soil water stress index (SWSI), an eco-hydrological drought indicator. Daily data was used from 2004–2014. Tukey honest significant difference tests were performed for pairwise comparisons; years which were not significantly different at $p < 0.05$ are represented by the same letter. In the boxplots, the thick line shows the median, the box extends to the upper and lower quartiles, dashed lines indicate the nominal range, and open circles indicate points which lie outside of the nominal range. The greater SWSI is, the lower soil water stress is.

Table A1. Regression coefficients between Rg-normalized ET or Rg-normalized WUE and soil water stress index (SWSI). Slopes with 95% confidence intervals (CI) and y-axis intercepts according to the SMA analysis are shown. Daily data over the 2004–2014 period were used.

Variables	Year	Slope	Slope CI		y-axis Intercept
			Lower	Upper	
Rg-Normalized ET and SWSI	2004	0.89	0.78	1.01	-0.13
	2005	0.46	0.39	0.54	-0.28
	2006	0.51	0.41	0.61	-0.05
	2007	0.65	0.55	0.77	-0.29
	2008	0.81	0.69	0.94	0.07
	2009	0.76	0.64	0.89	0.09
	2010	0.69	0.57	0.84	0.03
	2011	0.63	0.49	0.80	0.07
	2012	0.80	0.69	0.93	0.23
	2013	0.98	0.73	1.31	-0.70
	2014	0.86	0.70	1.04	0.04
Rg-Normalized WUE and SWSI	2004	-0.75	-0.87	-0.64	0.18
	2005	0.58	0.48	0.69	0.26
	2006	-0.40	-0.49	-0.33	-0.16
	2007	-0.61	-0.73	-0.52	0.22
	2008	-0.68	-0.82	-0.56	-0.35
	2009	-0.48	-0.58	-0.39	-0.01
	2010	-0.72	-0.89	-0.58	0.31
	2011	-0.57	-0.75	-0.44	0.17
	2012	-0.60	-0.73	-0.49	-0.04
	2013	-0.86	-1.15	-0.64	0.55
2014	0.67	0.54	0.83	-0.43	

Table A2. Comparison of slopes of Rg-Normalized ET or Rg-Normalized WUE and the soil water stress index (SWSI) for each year from 2004–2014 based on standardized major axis (SMA) regression analyses.

Variables	Comparison of Slopes											
	2004	2005	2006	2007	2008	2009	2010	2011	2012	2013	2014	
Rg-Normalized ET	2004											
	2005	***										
	2006	***	-									
	2007	-	-									
	2008	-	***	**								
	2009	-	***	-								
	2010	-	-	-								
	2011	-	-	-								
	2012	-	***	*								
	2013	-	***	**								
	2014	-	***	**								
Rg-Normalized WUE	2004											
	2005	-										
	2006	***										
	2007	-	-									
	2008	-	-	**								
	2009	***	-	-								
	2010	-	-	***								
	2011	-	-	-								
	2012	-	-	-								
	2013	-	-	***								
	2014	-	-	**								

Significant differences between SMA slopes for different years are shown by (*) and (-) symbols. Significance level: *, 0.01–0.05; **, 0.01–0.001; ***, <0.001; (-), non-significant relationships.

References

- Von Randow, C.; Zeri, M.; Restrepo-Coupe, N.; Muza, M.N.; de Gonçalves, L.G.G.; Costa, M.H.; Araujo, A.C.; Manzi, A.O.; da Rocha, H.R.; Saleska, S.R.; et al. Interannual variability of carbon and water fluxes in Amazonian forest, Cerrado and pasture sites, as simulated by terrestrial biosphere models. *Agric. For. Meteorol.* **2013**, *182–183*, 145–155. [[CrossRef](#)]
- Duffy, P.B.; Brando, P.; Asner, G.P.; Field, C.B. Projections of future meteorological drought and wet periods in the Amazon. *Proc. Natl. Acad. Sci. USA* **2015**, *112*, 13172–13177. [[CrossRef](#)]
- Cox, P.M.; Betts, R.A.; Collins, M.; Harris, P.P.; Huntingford, C.; Jones, C.D. Amazonian forest dieback under climate-carbon cycle projections for the 21st century. *Theor. Appl. Climatol.* **2004**, *78*, 137–156. [[CrossRef](#)]
- Poulter, B.; Hattermann, F.; Hawkins, E.; Zaehle, S.; Sitch, S.; Restrepo-Coupe, N.; Heyder, U.; Cramer, W. Robust dynamics of Amazon dieback to climate change with perturbed ecosystem model parameters. *Glob. Chang. Biol.* **2010**, *16*, 2476–2495. [[CrossRef](#)]
- Saleska, S.R.; Didan, K.; Huete, A.R.; Da Rocha, H.R. Amazon forests green-up during 2005 drought. *Science* **2007**, *318*, 612. [[CrossRef](#)] [[PubMed](#)]
- Phillips, O.L.; Aragão, L.E.O.C.; Lewis, S.L.; Fisher, J.B.; Lloyd, J.; López-González, G.; Malhi, Y.; Monteagudo, A.; Peacock, J.; Quesada, C.A.; et al. Drought sensitivity of the amazon rainforest. *Science* **2009**, *323*, 1344–1347. [[CrossRef](#)] [[PubMed](#)]
- Bonal, D.; Burban, B.; Stahl, C.; Wagner, F.; Hérault, B. The response of tropical rainforests to drought—Lessons from recent research and future prospects. *Ann. For. Sci.* **2016**, *73*, 27–44. [[CrossRef](#)] [[PubMed](#)]
- Wang, K.C.; Dickinson, R.E. A review of global terrestrial evapotranspiration: Observation, modeling, climatology, and climatic variability. *Rev. Geophys.* **2012**, *50*. [[CrossRef](#)]
- Fisher, R.A.; Williams, M.; da Costa, A.L.; Malhi, Y.; da Costa, R.F.; Almeida, S.; Meir, P. The response of an Eastern Amazonian rain forest to drought stress: Results and modelling analyses from a throughfall exclusion experiment. *Glob. Chang. Biol.* **2007**, *13*, 2361–2378. [[CrossRef](#)]

10. Costa, M.H.; Biajoli, M.C.; Sanches, L.; Malhado, A.C.M.; Hutyrá, L.R.; Da Rocha, H.R.; Aguiar, R.G.; De Araújo, A.C. Atmospheric versus vegetation controls of Amazonian tropical rain forest evapotranspiration: Are the wet and seasonally dry rain forests any different? *J. Geophys. Res. Biogeosci.* **2010**, *115*, 1–9. [[CrossRef](#)]
11. Carswell, F.E.; Costa, A.L.; Palheta, M.; Malhi, Y.; Meir, P.; Costa, J.D.P.R.; Ruivo, M.D.L.; Leal, L.D.S.M.; Costa, J.M.N.; Clement, R.J.; et al. Seasonality in CO₂ and H₂O flux at an eastern Amazonian rain forest. *J. Geophys. Res. D Atmos.* **2002**, *107*, 8076. [[CrossRef](#)]
12. Hasler, N.; Avissar, R. What controls evapotranspiration in the Amazon basin? *J. Hydrometeorol.* **2007**, *8*, 380–395. [[CrossRef](#)]
13. Da Rocha, H.R.; Manzi, A.O.; Cabral, O.M.; Miller, S.D.; Goulden, M.L.; Saleska, S.R.; Coupe, N.R.; Wofsy, S.C.; Borma, L.S.; Artaxo, R.; et al. Patterns of water and heat flux across a biome gradient from tropical forest to savanna in Brazil. *J. Geophys. Res. Biogeosci.* **2009**, *114*. [[CrossRef](#)]
14. Kim, Y.; Knox, R.G.; Longo, M.; Medvigy, D.; Hutyrá, L.R.; Pyle, E.H.; Wofsy, S.C.; Bras, R.L.; Moorcroft, P.R. Seasonal carbon dynamics and water fluxes in an Amazon rainforest. *Glob. Chang. Biol.* **2012**, *18*, 1322–1334. [[CrossRef](#)]
15. Maeda, E.E.; Ma, X.; Wagner, F.H.; Kim, H.; Oki, T.; Eamus, D.; Huete, A. Evapotranspiration seasonality across the Amazon Basin. *Earth Syst. Dyn.* **2017**, *8*, 439–454. [[CrossRef](#)]
16. Farquhar, G.D.; Ehleringer, J.R.; Hubick, K.T. Carbon isotope discrimination and photosynthesis. *Ann. Rev. Plant Physiol.* **1989**, *40*, 503–537. [[CrossRef](#)]
17. Hutyrá, L.R.; Munger, J.W.; Saleska, S.R.; Gottlieb, E.; Daube, B.C.; Dunn, A.L.; Amaral, D.F.; de Camargo, P.B.; Wofsy, S.C. Seasonal controls on the exchange of carbon and water in an Amazonian rain forest. *J. Geophys. Res. Biogeosci.* **2007**. [[CrossRef](#)]
18. Negrón Juárez, R.I.; Hodnett, M.G.; Fu, R.; Gouden, M.L.; von Randow, C. Control of dry season evapotranspiration over the Amazonian forest as inferred from observation at a Southern Amazon forest site. *J. Clim.* **2007**, *20*, 2827–2839. [[CrossRef](#)]
19. Fisher, J.B.; Malhi, Y.; Bonal, D.; Da Rocha, H.R.; De Araújo, A.C.; Gamo, M.; Goulden, M.L.; Rano, T.H.; Huete, A.R.; Kondo, H.; et al. The land-atmosphere water flux in the tropics. *Glob. Chang. Biol.* **2009**. [[CrossRef](#)]
20. Christoffersen, B.O.; Restrepo-Coupe, N.; Arain, M.A.; Baker, I.T.; Cestaro, B.P.; Ciais, P.; Fisher, J.B.; Galbraith, D.; Guan, X.; Gulden, L.; et al. Mechanisms of water supply and vegetation demand govern the seasonality and magnitude of evapotranspiration in Amazonia and Cerrado. *Agric. For. Meteorol.* **2014**, *191*, 33–50. [[CrossRef](#)]
21. Da Costa, A.C.L.; Rowland, L.; Oliveira, R.S.; Oliveira, A.A.R.; Binks, O.J.; Salmon, Y.; Vasconcelos, S.S.; Junior, J.A.S.; Ferreira, L.V.; Poyatos, R.; et al. Stand dynamics modulate water cycling and mortality risk in droughted tropical forest. *Glob. Chang. Biol.* **2018**. [[CrossRef](#)]
22. Huang, M.; Piao, S.; Sun, Y.; Ciais, P.; Cheng, L.; Mao, J.; Poulter, B.; Shi, X.; Zeng, Z.; Wang, Y. Change in terrestrial ecosystem water-use efficiency over the last three decades. *Glob. Chang. Biol.* **2015**. [[CrossRef](#)] [[PubMed](#)]
23. Brienen, R.J.W.; Wanek, W.; Hietz, P. Stable carbon isotopes in tree rings indicate improved water use efficiency and drought responses of a tropical dry forest tree species. *Trees* **2011**, *25*, 103–113. [[CrossRef](#)]
24. Yu, G.; Song, X.; Wang, Q.; Liu, Y.; Guan, D.; Yan, J.; Sun, X.; Zhang, L.; Wen, X. Water-use efficiency of forest ecosystems in eastern China and its relations to climatic variables. *New Phytol.* **2008**, *177*, 927–937. [[CrossRef](#)]
25. Aguilos, M.; Hérault, B.; Burban, B.; Wagner, F.; Bonal, D. What drives long-term variations in carbon flux and balance in a tropical rainforest in French Guiana? *Agric. For. Meteorol.* **2018**, 253–254. [[CrossRef](#)]
26. Bonal, D.; Bosc, A.; Ponton, S.; Goret, J.Y.; Burban, B.T.; Gross, P.; Bonnefond, J.M.; Elbers, J.; Longdoz, B.; Epron, D.; et al. Impact of severe dry season on net ecosystem exchange in the Neotropical rainforest of French Guiana. *Glob. Chang. Biol.* **2008**. [[CrossRef](#)]
27. Aubinet, M.; Grelle, A.; Ibrom, A.; Rannik, U.; Moncrieff, J.B.; Foken, T.; Kowalski, A.S.; Martin, P.H.; Berbigier, P.; Bernhofer, C.; et al. Estimates of the annual net carbon and water exchange of forests: The Euroflux methodology. *Adv. Ecol. Res.* **2000**, *30*, 113–175.
28. Wagner, F.; Hérault, B.; Stahl, C.; Bonal, D.; Rossi, V. Modeling water availability for trees in tropical forests. *Agric. For. Meteorol.* **2011**, *151*, 1202–1213. [[CrossRef](#)]

29. Kuglitsch, F.G.; Reichstein, M.; Beer, C.; Carrara, A.; Ceulemans, R.; Granier, A.; Janssens, I.A.; Koestner, B.; Lindroth, A.; Loustau, D.; et al. Characterisation of ecosystem water-use efficiency of European forests from eddy covariance measurements. *Biogeosci. Discuss.* **2008**, *5*, 4481–4519. [[CrossRef](#)]
30. Dekker, S.C.; Groenendijk, M.; Booth, B.B.B.; Huntingford, C.; Cox, P.M. Spatial and temporal variations in plant water-use efficiency inferred from tree-ring, eddy covariance and atmospheric observations. *Earth Syst. Dyn.* **2016**, *7*, 525–533. [[CrossRef](#)]
31. Yang, Y.; Guan, H.; Batelaan, O.; McVicar, T.R.; Long, D.; Piao, S.; Liang, W.; Liu, B.; Jin, Z.; Simmons, C.T. Contrasting responses of water use efficiency to drought across global terrestrial ecosystems. *Sci. Rep.* **2016**, *6*, 23284. [[CrossRef](#)] [[PubMed](#)]
32. Granier, A.; Bréda, N.; Biron, P.; Villette, S. A lumped water balance model to evaluate duration and intensity of drought constraints in forest stands. *Ecol. Model.* **1999**, *116*, 269–283. [[CrossRef](#)]
33. Kume, T.; Takizawa, H.; Yoshifuji, N.; Tanaka, K.; Tantasirin, C.; Tanaka, N.; Suzuki, M. Impact of soil drought on sap flow and water status of evergreen trees in a tropical monsoon forest in northern Thailand. *For. Ecol. Manag.* **2007**, *238*, 220–230. [[CrossRef](#)]
34. Xiao, J.; Sun, G.; Chen, J.; Chen, H.; Chen, S.; Dong, G.; Gao, S.; Guo, H.; Guo, J.; Han, S.; et al. Carbon fluxes, evapotranspiration, and water use efficiency of terrestrial ecosystems in China. *Agric. For. Meteorol.* **2013**. [[CrossRef](#)]
35. Boese, S.; Jung, M.; Carvalhais, N.; Reichstein, M. The importance of radiation for semi-empirical water-use efficiency models. *Biogeosciences* **2017**, *14*, 3015–3026. [[CrossRef](#)]
36. Bonal, D.; Ponton, S.; Le Thiec, D.; Richard, B.; Ningre, N.; Hérault, B.; Ogée, J.; Gonzalez, S.; Pignat, M.; Sabatier, D.; et al. Leaf functional response to increasing atmospheric CO₂ concentrations over the last century in two northern Amazonian tree species: An historical δ¹³C and δ¹⁸O approach using herbarium samples. *Plant Cell Environ.* **2011**, *34*, 1332–1344. [[CrossRef](#)] [[PubMed](#)]
37. Wagner, F.; Rossi, V.; Stahl, C.; Bonal, D.; Hérault, B. Water availability is the main climate driver of neotropical tree growth. *PLoS ONE* **2012**, *7*, e34074. [[CrossRef](#)]
38. Van der Molen, M.K.; Dolman, A.J.; Ciais, P.; Eglin, T.; Gobron, N.; Law, B.E.; Meir, P.; Peters, W.; Phillips, O.L.; Reichstein, M.; et al. Drought and ecosystem carbon cycling. *Agric. For. Meteorol.* **2011**, *151*, 765–773. [[CrossRef](#)]
39. Allen, C.D.; Macalady, A.K.; Chenchouni, H.; Bachelet, D.; McDowell, N.; Vennetier, M.; Kitzberger, T.; Rigling, A.; Breshears, D.D.; Hogg, E.H.; et al. A global overview of drought and heat-induced tree mortality reveals emerging climate change risks for forests. *For. Ecol. Manag.* **2010**, *259*, 660–684. [[CrossRef](#)]
40. Da Rocha, H.R.; Goulden, M.L.; Miller, S.D.; Menton, M.C.; Pinto, L.D.; De Freitas, H.C. Seasonality of water and heat fluxes over a tropical forest in eastern Amazonia. *Ecol. Appl.* **2004**, *14*, 22–32. [[CrossRef](#)]
41. Baldocchi, D.; Falge, E.; Gu, L.; Olson, R.; Hollinger, D.; Running, S.; Anthoni, P.; Bernhofer, C.; Davis, K.; Evans, R.; et al. FLUXNET: A New tool to study the temporal and spatial variability of ecosystem-scale carbon dioxide, water vapor, and energy flux densities. *Bull. Am. Meteorol. Soc.* **2001**, *82*, 2415–2434. [[CrossRef](#)]
42. Stahl, C.; Hérault, B.; Rossi, V.; Burban, B.; Bréchet, C.; Bonal, D. Depth of soil water uptake by tropical rainforest trees during dry periods: Does tree dimension matter? *Oecologia* **2013**, *173*, 1191–1201. [[CrossRef](#)] [[PubMed](#)]
43. Nepstad, D.C.; De Carvalho, C.R.; Davidson, E.A.; Jipp, P.H.; Lefebvre, P.A.; Negreiros, G.H.; Da Silva, E.D.; Stone, T.A.; Trumbore, S.E.; Vieira, S. The role of deep roots in the hydrological and carbon cycles of Amazonian forests and pastures. *Nature* **1994**. [[CrossRef](#)]
44. Lee, J.-E.; Boyce, K. Impact of the hydraulic capacity of plants on water and carbon fluxes in tropical South America. *J. Geophys. Res.* **2010**. [[CrossRef](#)]
45. Xiao, X.; Zhang, Q.; Saleska, S.; Hutyrá, L.; De Camargo, P.; Wofsy, S.; Frolking, S.; Boles, S.; Keller, M.; Moore, B. Satellite-based modeling of gross primary production in a seasonally moist tropical evergreen forest. *Remote Sens. Environ.* **2005**, *94*, 105–122. [[CrossRef](#)]
46. Wagner, F.H.; Hérault, B.; Bonal, D.; Stahl, C.; Anderson, L.O.; Baker, T.R.; Becker, G.S.; Beeckman, H.; Souza, D.B.; Botosso, P.C.; et al. Climate seasonality limits leaf carbon assimilation and wood productivity in tropical forests. *Biogeosciences* **2016**, *13*, 2537–2562. [[CrossRef](#)]
47. Stahl, C.; Burban, B.; Wagner, F.; Goret, J.-Y.; Bompuy, F.; Bonal, D. Influence of Seasonal Variations in Soil Water Availability on Gas Exchange of Tropical Canopy Trees. *Biotropica* **2013**, *45*, 155–164. [[CrossRef](#)]

48. Maréchaux, I.; Bonal, D.; Bartlett, M.K.; Burban, B.; Coste, S.; Courtois, E.A.; Dulormne, M.; Goret, J.-Y.; Mira, E.; Mirabel, A.; et al. Dry-season decline in tree sapflux is correlated with leaf turgor loss point in a tropical rainforest. *Funct. Ecol.* **2018**, *32*, 2285–2297. [[CrossRef](#)]
49. Chaves, M.M.; Maroco, J.P.; Pereira, J.S. Understanding plant responses to drought—from genes to the whole plant. *Funct. Plant Biol.* **2003**, *30*, 239–264. [[CrossRef](#)]



© 2018 by the authors. Licensee MDPI, Basel, Switzerland. This article is an open access article distributed under the terms and conditions of the Creative Commons Attribution (CC BY) license (<http://creativecommons.org/licenses/by/4.0/>).